

Repository Istituzionale dei Prodotti della Ricerca del Politecnico di Bari

Non-linear analysis of RC masonry-infilled frames using the SLaMA method: part 2—parametric analysis and validation of the procedure

This is a post print of the following article

Original Citation:
Non-linear analysis of RC masonry-infilled frames using the SLaMA method: part 2—parametric analysis and validation of the procedure / Gentile, R., Pampanin, S., Raffaele, D., Uva, G.. - In: BULLETIN OF EARTHQUAKE ENGINEERING. - ISSN 1570-761X. - STAMPA. - 17:6(2019), pp. 3305-3326. [10.1007/s10518-019-00584-6]

Availability:
This version is available at http://hdl.handle.net/11589/176238 since: 2022-06-08

Published version
DOI:10.1007/s10518-019-00584-6

Publisher:

Terms of use:

(Article begins on next page)

17 November 2026

Non-linear analysis of RC masonry-infilled frames using the SLaMA method: part 2—parametric analysis and validation of the procedure

Roberto Gentile[1] · Stefano Pampanin[2] · Domenico Raffaele[3] · Giuseppina Uva[3]

1 *Institute for Risk and Disaster Reduction, University College London, London, UK*
2 *Department of Structural and Geotechnical Engineering, University of Rome "La Sapienza", Rome, Italy*
3 *Department of Civil, Environmental and Landscape, Building Engineering and Chemistry, Polytechnic University of Bari, Bari, Italy*

Abstract

Infill walls have significant effects on the global force–displacement curve of Reinforced Concrete (RC) frames, and possibly on the outcome of a seismic performance assessment. Therefore, it is paramount to explicitly consider their presence. An analytical procedure to derive the non-linear static force–displacement curve of infilled frame structures, within the Simple Lateral Mechanism Analysis (SLaMA) framework, has been presented in a companion paper (part 1). In this paper, the proposed procedure is applied to 72 case study infilled frames with different geometry (two, four, six stories; two, four bays), capacity and configuration of the RC members, strength and the distribution of the infills. The resulting capacity curves are compared to refined numerical pushover analyses. The observed satis- fying match demonstrates the accuracy and reliability of the proposed procedure.

Keywords Seismic assessment · Displacement-based assessment · Reinforced concrete · Infilled frame structures · Non-linear analysis

1 Introduction

The presence of infill walls has a significant influence on the non-linear response of a wide range of structural typologies. For RC frames, recent experimental and numerical stud- ies demonstrated such effects at both at local (distribution of the internal actions on the members, Santhi et al. 2005; Cavaleri and Di Trapani 2015) and global level (global capacity curve, Magenes and Pampanin 2004; Chrysostomou and Asteris 2012; Furtado et al. 2018a). These also include the out-of-plane response of the infills (Ricci et al. 2018; Fur- tado et al. 2018b) and the presence of openings (Asteris et al. 2011, 2012, 2016). Such effects are also demonstrated with post-earthquake damage reconnaissance (e.g. De Luca et al. 2018).

Such effects might considerably influence the outcome of the seismic assessment of infilled frame structures. Therefore, it is paramount to explicitly consider the presence of infills in seismic analyses. Although the presence of infills can be consid- ered in non-linear numerical analyses, their accuracy strongly depends on the ability of the adopted modelling strategy to properly capture the plastic mechanism of the structure. Therefore, simplified analytical procedures are needed to identify the structural weaknesses and their influence on the structural behaviour.

A number of analytical procedures are available in the literature to indirectly

account for the influence of the infills on the seismic behaviour. For instance, Landi et al. (2016) do so by using specific ductility-damping law valid for infilled RC frame buildings. Alter- natively, Cardone and Flora (2017) account for infills by scaling the displacement profile of the bare frame using calibrated factors. Conversely, an analytical procedure to explicitly consider the infills and derive the non-linear static capacity curve of masonry-infilled RC frame structures has been proposed in a companion paper (Gentile et al. 2019b), within the framework of the Simple Lateral Mechanism Analysis (SLaMA, Priestley and Calvi 1991; Park 1995; Priestley 1997; NZSEE 2017; Gentile 2017; Gentile et al. 2017, 2018; Gentile et al. 2019a, b; Del Vecchio et al. 2018). Such a procedure is summarised in Fig. 1.

In this paper, the proposed SLaMA methodology is tested to evaluate its reliability in providing a first estimation of the non-linear capacity curve of masonry-infilled frames. The SLaMA procedure is herein applied to 72 infilled frame case studies with regular geom- etry. The database includes buildings with two, four or six storeys, and two or four bays. A range of configurations for the RC members is considered, varying the strength and defor- mation capacity of beams and columns and the detailing in beam-column joints, therefore leading to different expected plastic mechanisms. Both uniformly infilled and "pilotis" configurations (infills missing at the ground storey) are considered, also accounting for two strength levels of the infill panels, which are somehow representative of external or internal infills.

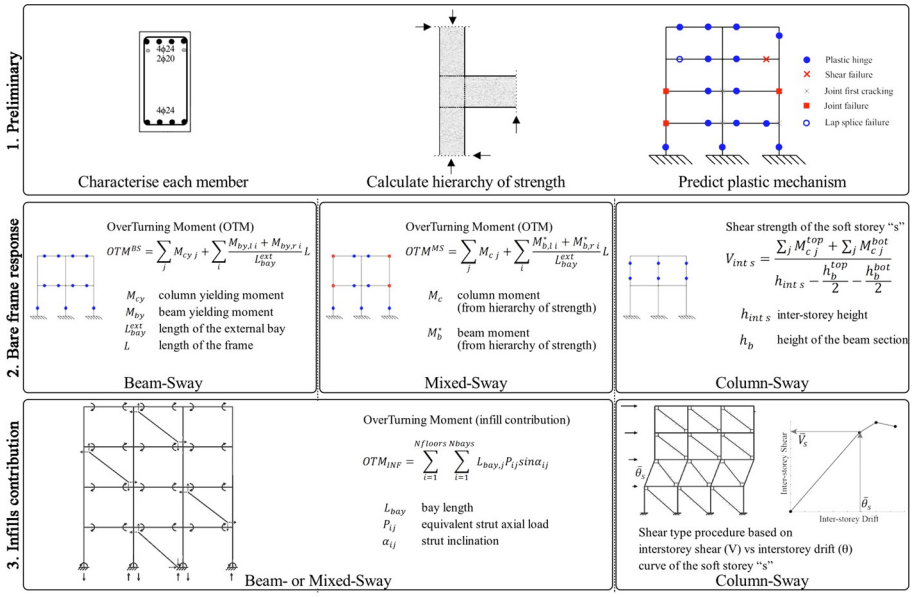


Fig. 1 SLaMA procedure for masonry-infilled RC frames

For each case in the database, the SLaMA-based capacity curve is compared with the results of a refined numerical pushover analysis, adopting a state-of-the-art modelling strat- egy. The good match obtained, both in terms of predicted failure mechanism and capacity curve itself, validates the proposed SLaMA

procedure for infilled frames, which is proved to be a reliable method to assess the capacity of such structures, in a simple yet accurate way.

2 Database of case studies

The 72 infilled frame case studies included in the database represent the longitudinal frames of the buildings depicted in Fig. 2. The transverse frames are not assessed in this paper, and their influence on the lateral capacity of the longitudinal frames is reasonably neglected.

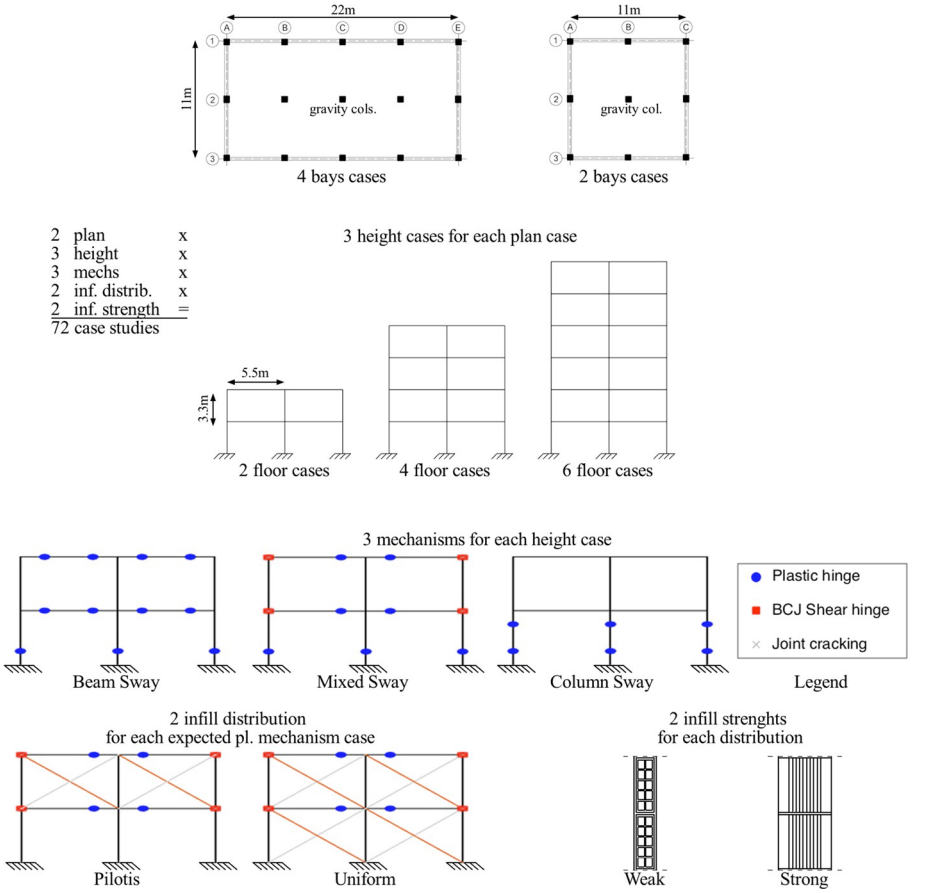


Fig. 2 Database of case studies

Case studies with two or four 5.5 m-long bays are considered, analysing 2-, 4- and 6-storey cases (the inter-storey height is equal to 3.3 m). For each geometrical configu- ration, three different solutions are adopted for the detailing of the RC members, leading to three different expected plastic mechanisms: Beam-Sway (all beams and the base columns yield), Mixed-Sway (combination of joint shear failures with beam and/or column flexure, shear or lap-splice failures) and Column-Sway (soft storey mechanism at the ground

storey). Therefore, for each combination of the above-mentioned parameters, two different distributions of the infills are considered: uniform distribution and "pilotis". Finally, two levels of strength for the infills are considered, representing external and internal partitions, and called *strong* and *weak*, respectively. It is worth mentioning that the effect of openings in the infills is outside the scope of this work and requires further investigations. According to simplified methods, infills with openings may be characterised by a calibrated reduc- tion of stiffness and strength when compared to the full panels (Holmes 1961). Therefore, although not specifically considered in this paper, the variability related to openings is deemed to be indirectly considered in this database by considering two different stiffness/ strength levels for the infills. The combination of the above-mentioned parameters leads to a set of 72 case studies, represented in Fig. 2.

2.1 Load analysis, material properties and detailing of the members

For the load analysis, a concrete density equal to ρ_c = 25 kN/m3 is considered, together with a superimposed dead load equal to D_{sdl} = 0.5 kN/m2 and a live load Q = 3 kN/m2 (ϕ_e = 0.3 reduction factor). The calculated seismic weight of one storey, constant along the height, is approximately equal to 1035 kN and 2017 kN for the 2- and 4-bays buildings, respectively. The axial load on the columns is calculated based on tributary areas.

The chosen mechanical characteristics of the materials are meant to be representative of typical existing buildings (e.g. NZSEE 2017, appendices C5E.1–C5E.3). Concrete compressive strength is equal to f_c = 25 MPa. Mander et al. (1988) is used for the characterisa- tion, conservatively adopting 0.02 as an upper bound for confined concrete ultimate strain.

The reinforcing steel (deformed bars) in the beams is characterised by f_y = 300 MPa and f_u = 390 MPa, respectively for yielding and ultimate stress. A stronger steel is used for col- umns, consistently with a common practice in existing buildings (e.g. in building #39 in Pampanin et al. 2012). King et al. (1986) is adopted for the characterisation, considering an ultimate strain equal to $_{su}$ = 0.06 and an elastic modulus equal to E_s = 200 GPa. It is worth mentioning that no factoring is adopted for the properties of the materials.

The detailing of the RC members for each case study is summarised in Fig. 3. It is worth mentioning that shear design is provided according to the ductility-dependent shear strength formulation by Kowalsky and Priestley (2000). More information regarding the detailing are given in Gentile et al. (2019a) and Gentile (2017), together with a detailed analysis of the plastic mechanisms and capacity curves of the bare frame configurations.

Two different configurations of the infills are considered (Fig. 2), which are meant to rep- resent typical configurations in existing buildings (Morandi et al. 2011). The *weak* typology is composed by 8 cm-wide horizontally hollowed clay bricks (60% void ratio) with 1 cm plaster on both sides. The *strong* typology is composed by 30 cm-wide vertically hollowed clay bricks (50% void ratio). The relevant mechanical properties are listed in Table 1. Finally, Table 2 shows the properties of two examples equivalent struts, characterised according to Bertoldi et al. (1993), which considers different failure mechanisms of the infills,

including crushing at the centre or near the corners, sliding shear or diagonal tension. Such characterisation, detailed on a step-by step basis in Gentile (2017) and resumed in the companion paper (part 1), is per- formed considering two 30 cm-deep, 60 cm-wide columns and two 60 cm-tall, 30 cm-deep beams using their secant-to-yielding moments of inertia. For both beams and columns, the longitudinal and transverse reinforcement ratios are equal to 0.6% and 0.75%, respectively.

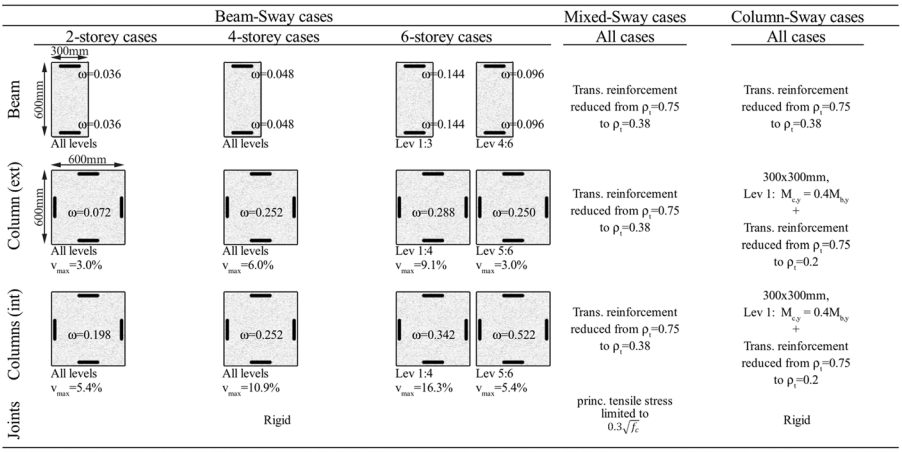


Fig. 3 Detailing of the RC members

Table 1 Mechanical properties of

MPa	f_{wh}	f_{wv}	f_{wu}	f_{ws}	E_{wh}	E_{wv}	G
Weak	1.18	2.02	0.44	0.55	991	1873	1089
Strong	1.5	3.51	0.3	0.36	1050	3240	1089

where f_{wh} and f_{wv} are the horizontal and vertical compressive strengths, f_{wu} is the cohesion of the mortar beds, f_{ws} is the shear strength for diagonal compression, E_{wh} and E_{wv} are the horizontal and vertical elastic moduli and G is the shear modulus

Table 2 Mechanical properties of two examples equivalent struts

	H_{int} (m)	L_{bay} (m)	d_w (m)	t_w (m)	A_{strut} (m^2)	K_{strut} (kN/m)	$E_{w\theta}$(MPa)	P_{max} (kN)
Weak	3.30	5.50	6.41	0.10	0.25	1,335,751	1271	184.6
Strong	3.30	5.50	6.41	0.30	0.47	1,443,100	1324	362.5

where d_w is the length of the strut, t_w is its width, A_{strut} is its area, $K_{strut} = \frac{E_{w\theta} A_{strut}}{d_w}$ is its stiffness, $E_{w\theta}$ is the inclined elastic modulus of the strut and P_{max} is the peak axial load

3 Numerical modelling strategy

Each case in the database is studied by means of a numerical pushover analysis

using the non-linear FEM software Ruaumoko (Carr 2016). The analyses are conducted in displace- ment control, applying a linear force profile and neglecting P-Delta effects. Rigid in-plane floor diaphragm constraint is assumed, together with fixed boundary conditions at the base of the columns. The analyses are terminated when the first member in the system reaches its ultimate displacement capacity.

As discussed in detail in the companion paper (part 1), both micro-modelling (Asteris et al. 2013) or macro-modelling techniques (Crisafulli et al. 2000) are available in the literature. The adopted modelling strategy (Fig. 4), validated against experimental tests (Magenes and Pampanin 2004), is based on a lumped plasticity approach. Mono-dimen- sional Giberson elements (Sharpe 1976) are adopted for beams and columns. The end sec- tions of the beams are characterised by a tri-linear Moment–Curvature (see Sect. 2.1 for the characterisation of the materials). Plastic hinge length is calculated according to Priest- ley et al. (2007), thus considering shear deformations and strain penetration (fixed-end rotation). Axial Load-Moment interaction diagram and plastic hinge length are used for columns. The software Cumbia (Montejo and Kowalsky 2007) is used for Moment–Cur- vature analyses the and the potential flange effect is accounted for with a 30% increase in the negative moment capacity of the beams. For beam and column members, rigid ends are used within the joint regions. To model the joint panel, the rigid ends are connected with non-linear lumped springs (two for each geometrical node of the frame). The non-linear behaviour of these springs is set consistently with the Equivalent Column Moment-Joint Drift relationships (Gentile et al. 2019a).

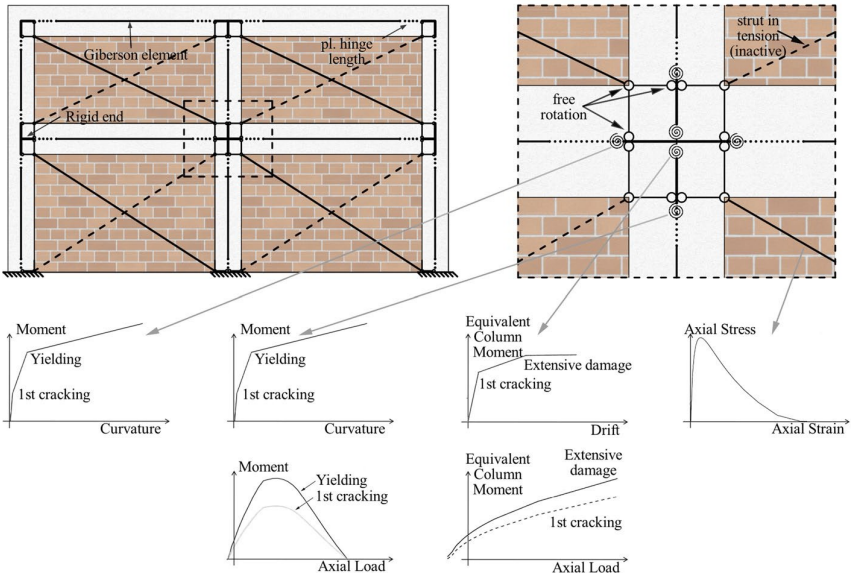


Fig. 4 Numerical modelling strategy

Infill panels are modelled using a modified version of the typical single equivalent strut approach. In such refinement, the pinned ends of each strut are

connected to the beam and column interfaces with the joint panels by means of two rigid arms (one horizontal, one vertical) able to sustain axial load only (Fig. 4). This allows to transfer the vertical and horizontal component of the axial load of the strut by means of shear demand for the beam and the column, respectively. When compared to the more commonly adopted method, in which the struts are connected to the centroid of the joints, this modified version allows to better capture the increase in shear demand in the beam-column joints. It is worth not- ing, however, that the distribution of the internal actions due to the infill-frame interac- tion, which is outside the scope of this paper, is not properly captured with this strategy as much as with a micro-modelling approach. Although out of scope, a post-processing of the results would be needed to check for possible shear failure of the columns due to the infills. The peak axial load in the struts should be used to calculate the shear demand on the RC members, and this should be compared to their shear capacity (e.g. with the procedure in NZSEE 2017).

In the FEM software, the equivalent struts are modelled as spring elements. Their stiff- ness and strength are defined by the parameters A_{strut}, K_{strut}, E_w&, P_{max} (with definitions and examples in Table 2) and are characterised according to Bertoldi et al. (1993). The struts

are not able to sustain tension forces and the compression branch of their response is gov- erned by the Axial Stress-Axial Strain relationship proposed in Crisafulli (1997), explicitly modelled in Ruaumoko. To define the shape of such curve (shown in Fig. 4), only two parameters are needed: namely the strain at peak stress and ultimate strain. Based on the experimental results presented in Morandi et al. (2011), such parameters are set to 0.002 and 0.01, respectively, regardless of the strength of the infills.

4 Discussion of the results

For each case study, the capacity curve obtained with the proposed SLaMA proce- dure is compared to the numerical pushover analysis, calculating the percentage error ($Err = \frac{SLaMA - P.O.}{P.O.}$) for a number of significant parameters. Namely, the initial stiffness, peak base shear, ultimate base shear and displacement are selected. Those are deemed the most influencing parameters for the assessment based on the most common procedures non-linear static analyses (N2 method, EC8 2005, Capacity Spectrum method, ATC 1996, percentage of New Building Standard, NZSEE 2017). For three selected case studies, the results are described in detail (Figs. 5, 6, 7). The error trends for the entire database are resumed in Fig. 8 and Table 3, together with a report of the Coefficient of Variation (CoV) in Table 4. Finally, the force–displacement results are shown in Fig. 9 and Table 5. The first natural period for the analysed case studies ranges between $T^{inf} = 0.11$ s and $T^{inf} = 1.00$ s

while the corresponding range for the bare structures is $T^{b} = (0.23$ s, 1.29 s). The infill-to- bare period ratios for the entire database are shown in Table 5. It is worth mentioning that detailed results for each case study are shown in Gentile 2017.

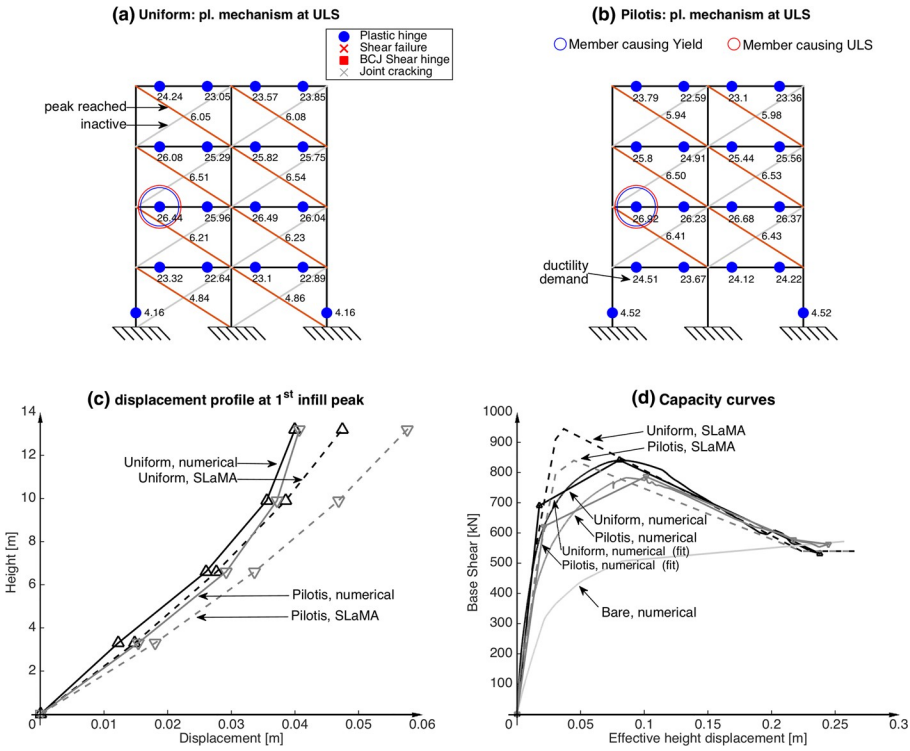


Fig. 5 SLaMA/numerical comparison for the Beam-Sway, weak infills, 2-bays 4-storeys case: uniform vs. pilotis infills distribution

To calculate the percentage error, the numerical capacity curves are represented in a multi-linear form. The point on the curve for which the first infill loses linearity in the response (one-third of the strain at peak stress) is used to define the initial stiffness. The curve is bi-linearised up to the peak response using the "equal energy" rule. In general, other two points are added to the multi-linear representation: the one for which the contri- bution of all the infills vanishes (if this point exists), and the ultimate point of the curve. Finally, it is worth mentioning that a linear force profile is assumed in the numerical anal- yses and in SLaMA (Column-Sway only; since for Beam-Sway and Mixed-Sway case studies a plastic mechanism approach is used, and no assumption is needed for the force profile).

4.1 Detailed comparison on selected cases

Three case studies are selected for a detailed comparison of the results: a Beam-Sway, a Mixed-Sway and a Column-Sway. The first of them is the 2-bays, 4-storeys, Beam-Sway frame with strong infills. Both the uniform and pilotis distributions are commented here.

Table 3 SLaMA versus numerical error

Case study				Error (%)				Case study				Error (%)			
				K_y	$V_{B,max}$	d_u	$V_{B,u}$					K_y	$V_{B,max}$	d_u	$V_{B,u}$
BS	W	Un	2b2s	– 52.4	1.4	15.6	– 5.6	MS	S	Un	2b2s	– 30.9	11.2	– 1.1	5.7
			2b2s	– 10.3	10.9	31.1	– 1.1				2b2s	1.1	15.2	20.7	– 5.6
			2b6s	– 1.7	13.2	14.8	– 13.6				2b6s	3.9	21.9	1.7	5.5
			4b2s	– 17.3	9.9	23.0	– 9.1				4b2s	– 10.3	9.0	11.8	– 6.2
			4b4s	– 9.9	11.4	23.5	– 2.7				4b4s	– 2.3	16.8	28.6	– 4.4
			4b6s	– 4.4	13.3	18.2	– 17.0				4b6s	0.7	21.8	4.1	5.1
		Pil	2b2s	– 7.3	– 2.0	9.1	– 6.0			Pil	2b2s	24.6	41.2	18.3	22.1
			2b4s	– 1.6	4.6	27.5	– 6.6				2b4s	28.1	12.9	34.8	– 4.5
			2b6s	1.7	12.8	13.6	– 13.0				2b6s	15.3	24.8	7.1	10.3
			4b2s	– 7.6	– 2.8	9.1	– 6.3				4b2s	26.3	0.3	5.1	– 10.8
			4b4s	3.1	10.0	23.5	– 5.0				4b4s	33.1	19.9	43.1	1.3
			4b6s	– 1.3	13.1	18.8	– 17.8				b6s	12.1	27.1	10.6	12.2
	S	Un	2b2s	– 25.5	13.3	13.0	– 5.6	CS	W	Un	2b2s	– 38.8	– 24.9	23.3	– 20.8
			2b2s	– 4.9	13.5	25.1	– 21.2				2b2s	– 20.3	– 16.1	3.4	– 19.6
			2b6s	2.3	19.4	20.3	– 13.8				2b6s	12.2	3.3	– 12.1	– 3.3
			4b2s	– 13.4	7.7	25.7	– 0.1				4b2s	– 38.4	– 22.3	14.8	– 14.0
			4b4s	– 5.4	16.2	39.0	– 33.1				4b4s	– 26.2	– 16.1	6.6	– 19.5
			4b6s	– 2.0	18.6	35.9	– 20.6				4b6s	– 0.5	2.3	– 6.9	– 3.5
		Pil	2b2s	29.4	1.5	9.8	– 5.6			Pil	2b2s	– 50.9	– 0.5	31.6	– 0.5
			2b4s	21.5	13.1	28.8	– 25.4				2b4s	– 22.6	– 0.1	26.2	– 0.1
			2b6s	14.0	20.8	24.1	– 21.2				2b6s	5.5	0.0	7.5	0.0
			4b2s	2.3	– 10.7	20.3	– 18.1				4b2s	– 35.0	– 0.3	30.1	– 0.3
			4b4s	30.4	19.8	37.8	– 32.3				4b4s	– 28.8	– 0.1	27.7	– 0.1
			4b6s	9.6	22.2	43.3	– 22.1				4b6s	– 7.0	– 0.1	13.5	– 0.1

Table 3 (continued)

Case study				Error (%)				Case study			Error (%)			
				K_y	$V_{B,max}$	d_u	$V_{B,u}$				K_y	$V_{B,max}$	d_u	$V_{B,u}$
MS	W	Un	2b2s	– 40.8	11.6	– 5.3	11.3	S	Un	2b2s	– 23.1	– 3.1	25.2	– 12.3
			2b2s	– 7.0	14.8	13.7	– 0.1			2b2s	– 5.1	– 0.2	– 0.3	– 7.9
			2b6s	– 0.2	14.6	– 4.5	4.3			2b6s	14.1	2.8	– 14.7	– 5.4
			4b2s	– 14.9	10.5	3.6	– 1.9			4b2s	– 24.1	– 1.4	9.6	2.9
			4b4s	– 7.5	12.8	12.3	– 2.3			4b4s	– 13.7	– 0.4	4.0	– 8.2
			4b6s	– 1.5	14.5	– 2.6	3.9			4b6s	– 0.6	1.8	– 9.5	– 5.3
		Pil	2b2s	– 6.4	11.8	– 3.7	6.2		Pil	2b2s	– 51.3	– 0.5	32.0	– 0.5
			2b4s	1.7	6.5	13.4	– 3.6			2b4s	– 24.7	– 0.1	27.5	– 0.1
			2b6s	2.9	13.8	– 7.5	6.0			2b6s	– 2.5	0.0	14.0	0.0
			4b2s	10.5	2.2	0.5	– 3.5			4b2s	– 35.5	– 2.6	34.5	– 0.3
			4b4s	5.3	9.4	20.9	– 2.4			4b4s	– 30.5	– 0.1	30.0	– 0.1
			4b6s	1.4	16.0	– 7.3	7.2			4b6s	– 13.3	– 0.1	17.9	– 0.1

BS Beam-Sway, *MS* Mixed-Sway, *CS* Column-Sway, *W* "weak" infills, *S* "strong" infills, *Un* uniformly distributed, *Pil* pilotis, *b* bays, *s* storeys

Figure 5a, b show a snapshot of the numerical pushover analysis, related to the Ultimate Limit State (ULS) of the structure, in which the developed non-linearities are evident. The member causing the ULS is highlighted with a red circle.

For both the uniform and the pilotis cases, the plastic mechanism is global and the contribution of the infills vanishes. A global plastic mechanism is reported for all the Beam-Sway, pilotis cases in this database. As expected, this is related to the impossibility of single strut models to properly capture the geometric stiffening of the upper storeys, clearly caused by the infills, which "forces" the shear-type behaviour of first storey. For practical applications, it is strongly suggested to adopt the SLaMA Colum-Sway procedure to capture the soft-storey plastic mechanism in pilotis frames.

The presence and distribution of the infills has little influence on the displacement shape of the frame. This is evident Fig. 5c that shows the displacement profiles corresponding to the peak of the 1st infill (the contribution of the infills to the total base shear is approaching the maximum). This justifies the choice of using, in SLaMA, the same displacement shape used for bare frames.

In correspondence of the peak of the 1st infill, the effective height displacement is over-estimated by SLaMA (about 13.2%) for both uniform and pilotis cases. This happens for the Beam-Sway cases in the database, although it is deemed that this particular parameter is not crucial for the reliability of the SLaMA procedure.

Figure 5d shows the comparison of the SLaMA and numerical capacity curves for both distribution of the infills. The multi-linear representation of the numerical curves is also shown, along with the capacity of the related bare frame (calculated with a separate numerical analysis). The peak base shear is slightly over-estimated in SLaMA (4.6% and 10.9% for pilotis and uniform). This trend is confirmed in the majority of the Beam-Sway and Mixed-Sway cases in the database. Very good match is observed for the prediction of the initial stiffness (1.6% and 10.3% under-estimation for pilotis and uniform cases).

The contribution of the infills to the global base shear vanishes before the ULS is reached. This is observed for all the analysed Beam-Sway cases. The response of the system in the last branch of the capacity curve is particularly similar to the behaviour of an analogous bare frame, with almost the same ultimate displacement. For this reason, the error trends observed for Beam-Sway type bare frames by Gentile et al. (2019a) are deemed to be appropriate for the ultimate base shear and displacement. Basically, for the Beam-Sway cases the ultimate base shear is slightly under-estimated while the ultimate displacement is slightly over-estimated with respect to the numerical analysis.

The second selected case study is the Mixed-Sway, 4-bays 2-storeys pilotis frame, considering both the weak and strong infills. The plastic mechanism observed in the numerical pushover (Fig. 6a, b) is global, regardless of the strength of the infills (due to the single-strut approach). It is characterised by shear hinges for all the external joints, beam hinges for all the internal joints and base column hinges. Although all the infills exceed the peak response, the ULS of the frames is registered before their contribution vanishes. This is because the lowest "leeward" joint panel, with a particularly low displacement capacity, causes the ULS of the frame. Also in this case, the SLaMA Colum- Sway procedure is suggested to confirm (or disprove) the predicted plastic mechanism.

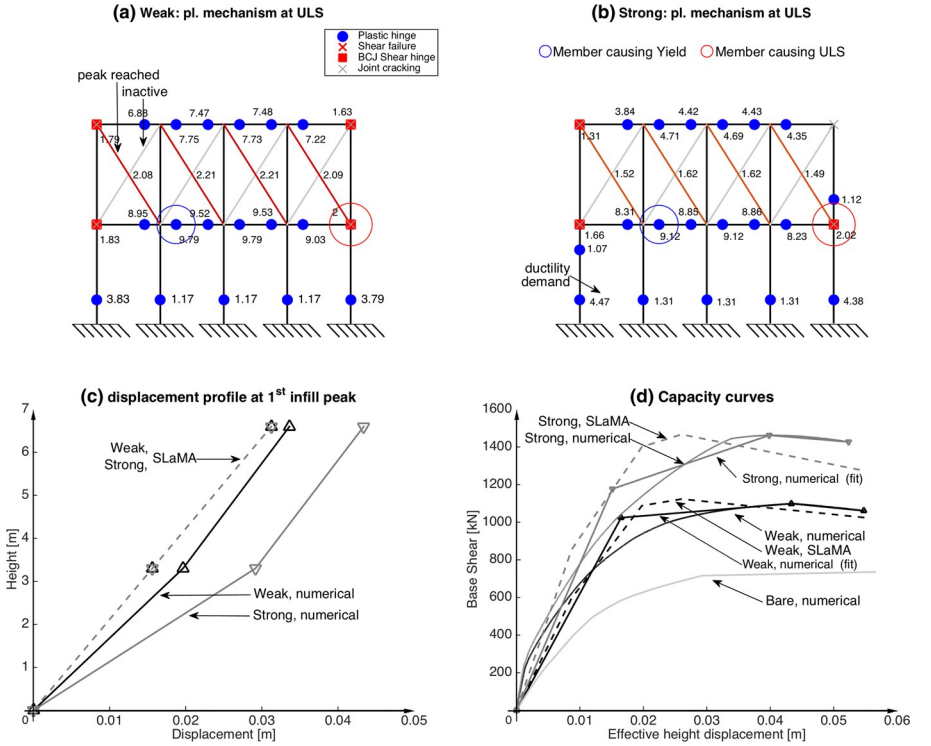


Fig. 6 SLaMA/numerical comparison for the Mixed-Sway, pilotis infills distribution, 4-bays 2-storeys case: weak versus strong infills

The displacement at the effective height related to the peak of the 1st infill (Fig. 6c) is under-estimated in SLaMA (9.5% and 30.8% for the weak and strong infills cases, respectively). Moreover, the related displacement profile in SLaMA is insensitive to the strength of the struts because, according to the proposed procedure, this is only based on the peak drift of the infills, which is set to 0.002. This under-estimation does not interfere on the good match between the SLaMA and the numerical pushover capacity curves (Fig. 6d).

A slight over-estimation can be observed with regard to the peak base shear (2.2% and 0.3% for weak and strong infills cases, respectively). The ultimate displacement is under-predicted by 0.5% and 5.1% for the weak and strong cases, respectively, while the corresponding under-prediction for the ultimate base shear is equal to 3.5% and 10.8%, respectively. Finally, the initial stiffness is over-predicted by 10.5% and 26.3% for the weak and strong infills cases, respectively.

A Column-Sway, 2-bays, 6-storeys frame with weak infills is selected for the last comparison, considering both the pilotis and uniform distributions of the infills. Since the columns at ground storey are weaker than the beams, a soft-storey mechanism at the first storey is observed. This plastic mechanism applies for both the uniform and pilotis distributions of the infills (Fig. 7a, b).

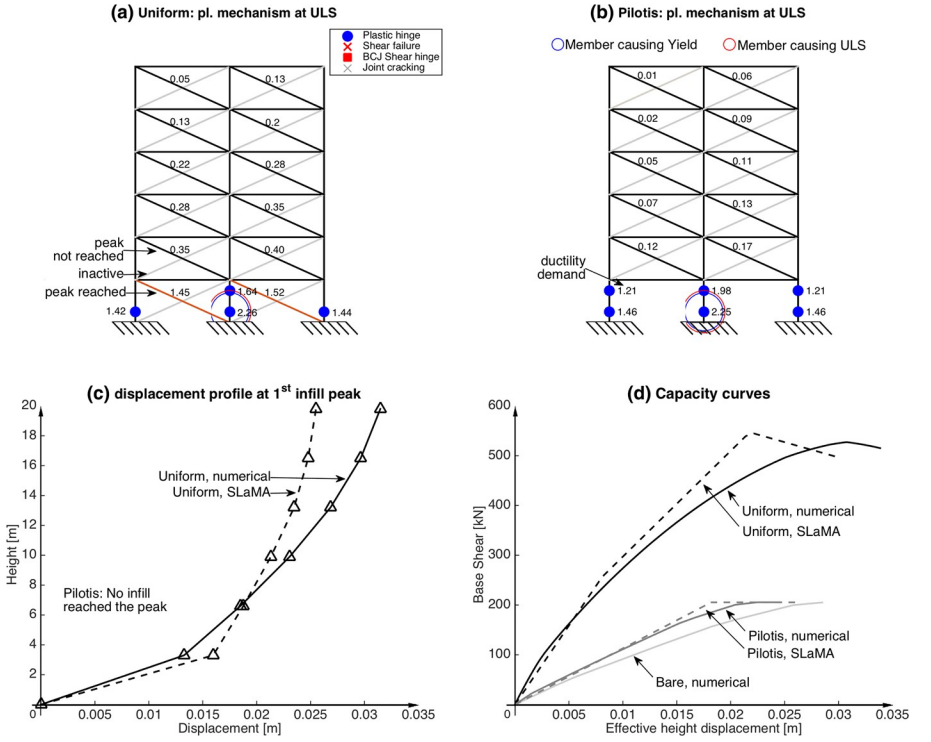


Fig. 7 SLaMA/numerical comparison for the Column-Sway, weak infills, 2-bays 6-storeys case: uniform versus pilotis infills distribution

The shear-type assumption of the Column-Sway SLaMA procedure leads, as expected, to a general under-estimation of the displacements. In Fig. 7c, this is shown for the displacement profile at the peak of the 1st infill. The related displacement at the effective height is under-predicted by 13.7%, while in the pilotis case no infill reaches the peak. The match between the SLaMA and numerical capacity curves is satisfactory (Fig. 7d), with a slight error on the peak base shear (+ 2.3% and − 0.1% for the uniform and pilotis cases) and an under-estimation of the initial stiffness (0.5% and 7.0%, respectively). Finally, the error on the ultimate displacement is − 6.9% and 13.5%, respectively for the uniform and pilotis case, while the base shear is under-predicted by 3.5% and 0.1%, respectively.

4.2 Accuracy of the proposed SLaMA procedure

In this Section, the accuracy of the proposed SLaMA is analysed by showing the SLaMA-to-numerical ratios for the entire database (Fig. 8) and therefore reporting the percentage error in Table 3. The capacity curves for the entire database are represented in Table 5, defined by means of the base shear and displacement at the significant points. Figure 9 shows the numerical capacity curves for the entire database.

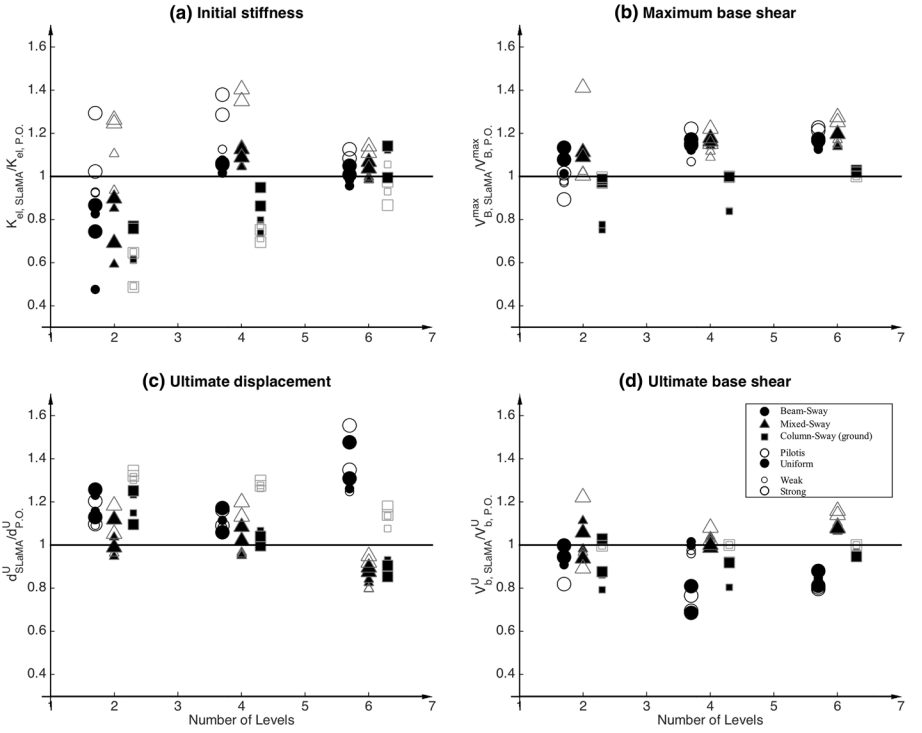


Fig. 8 SLaMA-to-numerical ratios of the selected parameters in the full database

The first analysed parameter is the initial stiffness (Fig. 8a), for which the magnitude and dispersion of the error reduces from (− 75%, 35%) for 2-storey cases to (− 15%, 15%) for 6-storey cases. For 2-storey cases, the relatively-higher infill contribution leads to a numerical pushover curve with a high initial curvature, also affecting the multi-linear fit. This is likely the source of the higher error in comparison with the initial linear branch of the SLaMA curve for less tall cases. For the Beam-Sway and Mixed-Sway mechanisms, the initial stiffness is under-estimated if the distribution of the infills is uniform while over- estimated if pilotis. For Column-Sway cases, the initial stiffness is under predicted for the vast majority of the cases with the magnitude of the error that reduces increasing the of the number of storeys.

The peak base shear (Fig. 8b) is predicted with a slight error (− 0.1%, 3.3%) for Col- umn-Sway cases, with the exception of a few case studies with weak infills. On the other hand, the error on this parameter falls in the interval (− 5%, 20%) for the majority of the Beam-Sway and Mixed-Sway cases. This slight over-prediction is produced assuming that the contribution of the frame in the infilled structure is equal to the bare frame response. This error is expected only for a global displacement close to the peak response.

The ultimate displacement (Fig. 8c) is over-estimated (about 20% maximum) for Beam-Sway cases with 2 or 4 storeys while the error is higher for 6-storeys cases (40% over-estimation, on average). For Mixed-Sway mechanisms, this error falls in the interval (− 20%, 20%): the ultimate displacement is over-predicted for 2- and 4-storeys cases while under-predicted for 6-storeys ones. The SLaMA-to-numerical error for this parameter is registered in the interval (− 20%, 35%) for the Column-Sway cases. An over-prediction is observed for all but the 6-storey cases, for which the ultimate displacement is under-pre- dicted with a 10% mean error.

The ultimate base shear (Fig. 8d) is under-predicted for all the analysed Beam-Sway cases (20%, on average) since the hardening of the members is conservatively not consid- ered in calculating the global-level calculations in SLaMA. This parameter is predicted within an error interval equal to (− 5%, 20%) the Mixed-Sway mechanisms, with more dis- persion observed for the 2-storeys cases. Finally, the error is close to zero for the pilotis Column-Sway cases while a slight under-prediction is observed for uniformly-infilled cases (20% maximum).

Finally, Table 4 shows an analysis the Coefficient of Variation (CoV) of the four inves- tigated parameters, both based on the results of the numerical pushover and the SLaMA analyses.

Table 4 Coefficient of variation for the four selected parameters, based on pushover analyses

	Coefficient of variation (CoV)			
	K_y	$V_{B,max}$	d_u	$V_{B,u}$
Beam Sway	0.61 (0.52)	0.61 (0.67)	0.96 (1.09)	0.68 (0.70)
Strong	0.55 (0.56)	0.73 (0.78)	0.96 (1.09)	0.78 (0.79)
Pilotis	0.59 (0.61)	0.67 (0.68)	0.88 (0.88)	0.66 (0.66)
Uniform	0.11 (0.19)	0.38 (0.44)	0.97 (1.13)	0.43 (0.46)
Weak	0.60 (0.50)	0.40 (0.47)	1.01 (1.13)	0.46 (0.50)
Pilotis	0.67 (0.56)	0.32 (0.39)	1.10 (1.24)	0.36 (0.41)
Uniform	0.53 (0.13)	0.28 (0.40)	0.84 (0.87)	0.32 (0.42)
Column Sway	0.67 (0.67)	0.69 (0.72)	0.95 (1.10)	0.71 (0.76)
Strong	0.64 (0.68)	0.69 (0.74)	1.00 (1.14)	0.71 (0.78)
Pilotis	0.52 (0.57)	0.68 (0.71)	0.98 (1.15)	0.69 (0.76)
Uniform	0.82 (0.85)	0.66 (0.65)	1.12 (1.25)	0.64 (0.67)
Weak	0.66 (0.65)	0.71 (0.73)	0.93 (1.09)	0.74 (0.78)
Pilotis	0.59 (0.65)	0.72 (0.72)	0.93 (0.88)	0.74 (0.75)
Uniform	0.12 (0.29)	0.26 (0.31)	0.93 (1.13)	0.27 (0.39)
Mixed Sway	0.79 (0.68)	0.52 (0.54)	0.99 (1.12)	0.58 (0.60)
Strong	0.61 (0.54)	0.36 (0.38)	0.99 (1.13)	0.44 (0.46)
Pilotis	0.68 (0.62)	0.30 (0.31)	1.09 (1.24)	0.38 (0.38)
Uniform	0.37 (0.17)	0.18 (0.24)	0.87 (0.87)	0.33 (0.39)
Weak	0.61 (0.63)	0.68 (0.72)	1.00 (1.14)	0.71 (0.72)
Pilotis	0.48 (0.50)	0.67 (0.70)	1.00 (1.15)	0.71 (0.71)
Uniform	0.79 (0.81)	0.61 (0.62)	1.11 (1.25)	0.60 (0.61)
Grand total	0.71 (0.64)	0.63 (0.68)	0.96 (1.09)	0.68 (0.71)

The results for SLaMA are reported in brackets

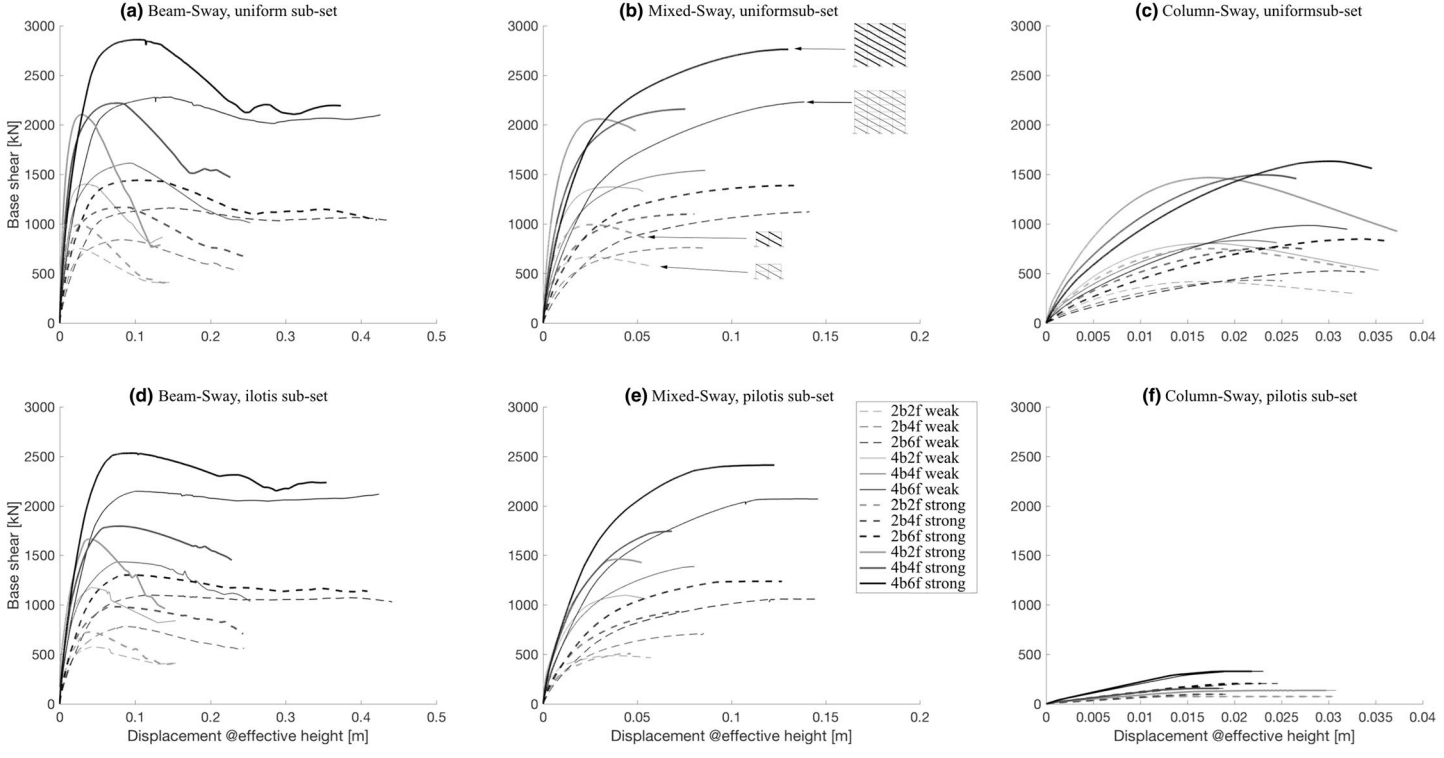


Fig. 9 Numerical pushover capacity curves for the entire database

Table 5 Significant points of the numerical pushover curve for the entire database. The results for SLaMA are reported in brackets

Case study				T_1^{inf}/T_1^b	Δ_y (cm)	Δ_{peak} (cm)	$\Delta_{inf=0}$ (cm)	Δ_u (cm)	V_{By} (kN)	$V_{B\ peak}$ (kN)	$V_{B\ inf=0}$ (kN)	V_{Bu} (kN)
BS	W	Un	2b2s	0.63	0.7 (2.0)	2.5 (2.5)	12.6 (13.0)	14.5 (16.8)	726.3 (730.5)	752.4 (763.0)	410.7 (387.0)	409.8 (387.0)
			2b4s	0.56	0.7 (2.0)	2.5 (2.5)	– (–)	5.8 (5.5)	640.1 (710.5)	665.3 (742.7)	– (–)	570.5 (634.9)
			2b6s	0.59	0.7 (0.6)	1.6 (1.6)	– (–)	3.3 (4.1)	346.4 (162.9)	419.2 (315.0)	– (–)	296.9 (235.1)
			4b2s	0.60	1.8 (3.0)	8.0 (3.7)	– (22.4)	23.8 (26.5)	690.4 (910.1)	841.2 (944.7)	– (539.7)	531.8 (539.7)
			4b4s	0.54	1.7 (3.0)	7.3 (3.7)	– (–)	8.5 (8.2)	626.1 (849.2)	761.6 (884.8)	– (–)	758.2 (787.2)
			4b6s	0.50	1.0 (0.7)	2.3 (2.1)	– (–)	2.5 (2.6)	349.3 (182.0)	433.1 (363.6)	– (–)	425.0 (341.9)
		Pil	2b2s	0.80	3.2 (6.6)	– (30.2)	43.7 (55.1)	988.3 (1309.4)	1163.0 (1309.4)	– (915.2)	1037.0 (915.2)	
			2b4s	0.66	2.9 (6.6)	14.0 (6.6)	– (–)	14.1 (11.6)	852.9 (1280.7)	1124.0 (1280.7)	– (–)	1123.0 (1197.1)
			2b6s	0.66	1.4 (0.8)	3.1 (2.2)	– (–)	3.4 (3.0)	392.4 (256.5)	527.1 (544.6)	– (–)	515.2 (498.1)
			4b2s	0.79	1.0 (2.0)	3.3 (2.5)	12.1 (13.0)	13.7 (16.8)	1277.9 (1477.0)	1401.0 (1539.6)	806.3 (787.5)	866.0 (787.5)
			4b4s	0.66	1.0 (2.0)	3.6 (2.5)	– (–)	5.3 (5.5)	1256.7 (1456.7)	1374.0 (1518.9)	– (–)	1329.0 (1303.2)
			4b6s	0.58	0.7 (0.6)	1.7 (1.6)	– (–)	3.5 (4.1)	682.9 (325.0)	804.3 (625.0)	– (–)	533.0 (458.6)
	S	Un	2b2s	0.49	1.8 (3.0)	9.2 (3.7)	23.7 (22.4)	25.3 (26.5)	1357.8 (1750.1)	1613.0 (1819.1)	1043.0 (1009.2)	1011.0 (1009.2)
			2b4s	0.45	1.8 (3.0)	8.6 (3.7)	– (–)	8.6 (8.2)	1289.2 (1687.3)	1540.0 (1758.3)	– (–)	1540.0 (1563.1)
			2b6s	0.44	0.9 (0.7)	2.1 (1.8)	– (–)	2.4 (2.6)	685.5 (358.0)	834.9 (700.3)	– (–)	811.6 (653.1)
			4b2s	0.47	3.2 (6.6)	14.7 (6.6)	– (30.2)	42.6 (55.1)	1989.8 (2567.6)	2280.0 (2567.6)	– (1779.0)	2100.0 (1779.0)
			4b4s	0.39	2.7 (6.6)	13.9 (6.6)	– (–)	13.9 (11.6)	1642.7 (2537.4)	2231.0 (2537.4)	– (–)	2231.0 (2370.1)
			4b6s	0.38	1.3 (0.8)	2.8 (2.2)	– (–)	3.2 (3.0)	759.4 (488.8)	984.1 (1006.8)	– (–)	947.0 (913.8)
		Pil	2b2s	0.73	1.3 (2.0)	4.2 (2.6)	13.0 (13.0)	15.4 (16.8)	463.5 (546.7)	576.7 (565.2)	401.8 (387.0)	411.6 (387.0)
			2b4s	0.59	1.3 (2.0)	3.7 (2.6)	– (–)	5.7 (5.5)	458.4 (526.5)	487.2 (544.9)	– (–)	466.3 (495.4)
			2b6s	0.55	1.1 (2.4)	3.0 (2.4)	– (–)	3.0 (4.0)	67.8 (74.5)	74.8 (74.5)	– (–)	74.8 (74.5)
			4b2s	0.74	2.1 (3.0)	10.1 (4.5)	21.7 (22.4)	24.5 (26.5)	621.5 (795.8)	786.8 (840.1)	577.8 (539.7)	562.8 (539.7)
			4b4s	0.56	2.0 (3.0)	8.4 (4.5)	– (–)	8.5 (8.2)	536.2 (735.3)	717.6 (780.2)	– (–)	707.3 (717.9)
			4b6s	0.50	1.3 (1.9)	1.9 (1.9)	– (–)	1.9 (2.4)	81.2 (96.5)	96.6 (96.5)	– (–)	96.6 (96.5)

Table 5 (continued)

Case study				T_1^{inf}/T_1^b	Δ_y (cm)	Δ_{peak} (cm)	$\Delta_{inf=0}$ (cm)	Δ_u (cm)	V_{By} (kN)	$V_{B\ peak}$ (kN)	$V_{B\ inf=0}$ (kN)	V_{Bu} (kN)
MS	W	Un	2b2s	0.61	3.3 (6.6)	11.4 (6.6)	– (30.2)	44.1 (55.1)	879.6 (1252.6)	1100.0 (1252. 6)	– (915.2)	1030.0 (915.2)
			2b4s	0.54	2.9 (6.6)	12.0 (6.6)	– (–)	14.6 (11.6)	747.2 (1224.0)	1066.0 (1224.0)	– (–)	1058.0 (1152.4)
			2b6s	0.58	1.5 (1.8)	2.2 (1.8)	– (–)	2.5 (2.6)	164.0 (205.4)	205.5 (205.4)	– (–)	205.5 (205.4)
			4b2s	0.58	1.3 (2.0)	4.2 (2.6)	13.0 (13.0)	15.4 (16.8)	945.9 (1108.4)	1177.0 (1143.9)	820.0 (787.5)	840.0 (787.5)
			4b4s	0.53	1.7 (2.0)	4.3 (2.6)	– (–)	5.5 (5.5)	1024.0 (1087.9)	1099.0 (1123.2)	– (–)	1061.0 (1024.2)
			4b6s	0.49	1.2 (2.4)	3.0 (2.4)	– (–)	3.1 (4.0)	105.1 (134.9)	135.3 (134.9)	– (–)	135.3 (134.9)
		Pil	2b2s	0.77	2.0 (3.0)	7.6 (4.5)	24.0 (22.4)	25.3 (26.5)	1084.4 (1521.4)	1434.0 (1609.9)	1095.0 (1009.2)	1035.0 (1009.2)
			2b4s	0.64	2.0 (3.0)	7.9 (4.5)	– (–)	8.0 (8.2)	1050.4 (1459.5)	1387.0 (1549.1)	– (–)	1387.0 (1424.5)
			2b6s	0.65	1.2 (1.9)	1.7 (1.9)	– (–)	1.9 (2.4)	139.9 (155.9)	156.0 (155.9)	– (–)	156.0 (155.9)
			4b2s	0.77	3.2 (6.6)	10.1 (6.6)	– (30.2)	42.4 (55.1)	1716.7 (2453.8)	2149.0 (2453.8)	– (1779.0)	2119.0 (1779.0)
			4b4s	0.64	3.0 (6.6)	13.3 (6.6)	– (–)	14.6 (11.6)	1567.6 (2423.8)	2071.0 (2423.8)	– (–)	2070.0 (2280.6)
			4b6s	0.57	1.4 (1.8)	2.3 (1.8)	– (–)	2.3 (2.6)	284.5 (328.4)	328.7 (328.4)	– (–)	328.7 (328.4)
	S	Un	2b2s	0.48	0.8 (2.0)	2.6 (2.5)	13.6 (13.0)	14.9 (16.8)	874.6 (1064.5)	993.4 (1125.4)	406.4 (387.0)	409.8 (387.0)
			2b4s	0.43	0.8 (2.0)	2.5 (2.5)	– (–)	5.6 (5.5)	947.3 (1044.6)	993.7 (1105.1)	– (–)	844.8 (893.3)
			2b6s	0.43	0.8 (0.6)	1.7 (1.7)	– (–)	3.3 (4.1)	657.2 (385.0)	751.5 (727.9)	– (–)	550.8 (483.1)
			4b2s	0.45	1.7 (3.0)	7.9 (3.7)	– (22.4)	25.0 (26.5)	1024.7 (1272.4)	1167.0 (1336.8)	– (539.7)	667.5 (539.7)
			4b4s	0.37	1.8 (3.0)	7.7 (3.7)	– (–)	8.0 (8.2v	954.5 (1210.7)	1099.0 (1276.9)	– (–)	1099.0 (1084.8)
			4b6s	0.37	1.2 (0.8)	2.5 (2.0)	– (–)	2.7 (2.7)	648.6 (405.1)	761.0 (759.6)	– (–)	746.6 (687.5)
		Pil	2b2s	0.71	2.8 (6.6)	10.1 (6.6)	– (30.2)	42.1 (55.1)	1240.1 (1691.5)	1441.0 (1691.5)	– (915.2)	1040.0 (915.2)
			2b4s	0.57	2.6 (6.6)	12.9 (6.6)	– (–)	13.3 (11.6)	1146.2 (1662.3)	1389.0 (1662.3)	– (–)	1387.0 (1497.6)
			2b6s	0.54	1.6 (1.0)	3.4 (2.4)	– (–)	3.7 (3.1)	688.7 (477.2)	847.8 (871.5)	– (–)	824.6 (780.1)
			4b2s	0.71	1.0 (2.0)	2.8 (2.5)	12.1 (13.0)	13.4 (16.8)	1921.7 (2147.7)	2102.0 (2264.3)	764.6 (787.5)	788.3 (787.5)
			4b4s	0.54	1.0 (2.0)	2.9 (2.5)	– (–)	4.9 (5.5)	1880.1 (2127.8)	2058.0 (2243.7)	– (–)	1941.0 (1820.1)
			4b6s	0.48	0.8 (0.6)	1.7 (1.7)	– (–)	3.7 (4.1)	1297.6 (769.5)	1467.0 (1446.8)	– (–)	925.5 (952.2)

Table 5 (continued)

Case study				T_1^{inf}/T_1^b	Δ_y (cm)	Δ_{peak} (cm)	$\Delta_{inf=0}$ (cm)	Δ_u (cm)	V_{By} (kN)	$V_{B\ peak}$ (kN)	$V_{B\ inf=0}$ (kN)	V_{Bu} (kN)
CS	W	Un	2b2s	0.23	1.7 (3.0)	7.0 (3.7)	– (22.4)	22.7 (26.5)	1962.7 (2474.9)	2221.0 (2603.4)	– (1009.2)	1470.0 (1009.2)
			2b4s	0.29	1.7 (3.0)	7.5 (3.7)	– (–)	7.5 (8.2)	1910.5 (2410.5)	2159.0 (2542.6)	– (–)	2159.0 (2158.4)
			2b6s	0.50	1.1 (0.8)	2.3 (2.0)	– (–)	2.7 (2.8)	1288.9 (804.6)	1495.0 (1488.7)	– (–)	1457.0 (1337.8)
			4b2s	0.21	2.7 (6.6)	10.1 (6.6)	– (30.2)	37.3 (55.1)	2472.0 (3332.0)	2860.0 (3332.0)	– (1779.0)	2193.0 (1779.0)
			4b4s	0.25	2.5 (6.6)	12.6 (6.6)	– (–)	13.0 (11.6)	2213.2 (3300.8)	2761.0 (3300.8)	– (–)	2761.0 (2971.3)
			4b6s	0.41	1.4 (1.0)	3.0 (2.3)	– (–)	3.5 (3.1)	1351.0 (932.1)	1632.0 (1661.6)	– (–)	1560.0 (1477.9)
		Pil	2b2s	0.69	1.6 (2.0)	3.9 (2.6)	– (13.0)	15.3 (16.8)	606.9 (702.1)	725.9 (736.9)	– (387.0)	409.8 (387.0)
			2b4s	0.76	1.0 (2.0)	4.7 (2.6)	– (–)	4.7 (5.5)	382.6 (682.1)	507.5 (716.6)	– (–)	507.5 (619.4)
			2b6s	0.85	1.1 (2.4)	3.0 (2.4)	– (–)	3.0 (4.0)	67.9 (74.5)	74.8 (74.5)	– (–)	74.8 (74.5)
			4b2s	0.71	2.2 (3.0)	7.3 (4.5)	– (22.4)	24.3 (26.5)	796.3 (1047.9)	980.7 (1130.2)	– (539.7)	705.3 (539.7)
			4b4s	0.77	2.3 (3.0)	7.2 (4.5)	– (–)	7.2 (8.2)	742.4 (987.0)	930.8 (1070. 3)	– (–)	930.8 (947.8)
			4b6s	0.83	1.2 (1.9)	1.8 (1.9)	– (–)	1.9 (2.4)	81.6 (96.5)	96.6 (96.5)	– (–)	96.6 (96.5)
	S	Un	2b2s	0.16	3.1 (6.6)	9.0 (6.6)	– (30.2)	40.8 (55.1)	1051.9 (1578.9)	1302.0 (1578.9)	– (915.2)	1138.0 (915.2)
			2b4s	0.23	3.0 (6.6)	11.1 (6.6)	– (–)	12.7 (11.6)	1000.1 (1549.8)	1238.0 (1549.8)	– (–)	1237.0 (1409.0)
			2b6s	0.40	1.4 (1.8)	2.0 (1.8)	– (–)	2.3 (2.6)	165.5 (205.4)	205.5 (205.4)	– (–)	205.5 (205.4)
			4b2s	0.14	1.5 (2.0)	3.9 (2.6)	– (13.0)	14.0 (16.8)	1413.5 (1420.9)	1665.4 (1487.3)	– (787.5)	962.1 (787.5)
			4b4s	0.19	1.5 (2.0)	4.0 (2.6)	– (–)	5.2 (5.5)	1176.8 (1400.6)	1462.0 (1466.6)	– (–)	1427.0 (1272.3)
			4b6s	0.31	1.6 (2.4)	2.6 (2.4)	– (–)	3.0 (4.0)	134.2 (134.9)	138.5 (134.9)	– (–)	135.3 (134.9)
		Pil	2b2s	0.69	2.4 (3.0)	7.5 (4.5)	– (22.4)	22.8 (26.5)	1557.4 (2026.0)	1795.0 (2190.1)	– (1009.2)	1452.0 (1009.2)
			2b4s	0.74	2.3 (3.0)	6.7 (4.5)	– (–)	6.8 (8.2)	1458.7 (1963.1)	1744.0 (2129.3)	– (–)	1744.0 (1884.3)
			2b6s	0.81	1.2 (1.9)	1.7 (1.9)	– (–)	1.8 (2.4)	140.2 (155.9)	156.0 (155.9)	– (–)	156.0 (155.9)
			4b2s	0.71	3.1 (6.6)	9.1 (6.6)	– (30.2)	35.4 (55.1)	2160.1 (3106.4)	2533.0 (3106.4)	– (1779.0)	2236.0 (1779.0)
			4b4s	0.76	2.9 (6.6)	11.6 (6.6)	– (–)	12.3 (11.6)	2006.4 (3075.5)	2412.0 (3075.5)	– (–)	2412.0 (2793.9)
			4b6s	0.80	1.3 (1.7)	2.1 (1.7)	– (–)	2.2 (2.6)	286.6 (328.4)	328.7 (328.4)	– (–)	328.7 (328.4)

BS Beam-Sway, *MS* Mixed-Sway, *CS* Column-Sway, *W* "weak" infills, *S* "strong" infills, *Un* uniformly distributed, *Pil* pilotis; *b* bays, *s* storeys, T_1^{inf}/T_1^b infill-to-bare 1st period ratio

The results show that, both on an aggregated or disaggregated basis, the CoV related to the analytical response is particularly similar to the one based on the refined numerical analyses. This indicates that, although error trends are observed between SLaMA and the numerical pushover results, the application of SLaMA does not introduce significant modification in the dispersion of the results.

5 Conclusions

An analytical procedure to calculate the non-linear capacity curve of masonry-infilled RC frames is proposed in a companion paper (Part 1) within the framework of the Simple Lateral Mechanism Analysis (SLaMA). The infilled frames SLaMA procedure is herein validated through the application to 72 RC infilled frames, considering 2 or 4 bays, 2, 4 or 6 storeys, and different expected plastic mechanisms. The dataset includes "Beam-Sway" cases, typical of new buildings, "Mixed-Sway" cases, characterised by a combination of joint panel failures and beams and columns flexural, shear or lap splice failures, "Column-Sway" cases, for which a soft storey at the ground is expected. "Weak" and "strong" infills are considered, representing internal and external partitions, together with two different distributions of the infills: uniform and pilotis.
The resulting SLaMA capacity curves are compared with refined numerical pusho- ver results to analyse the reliability and accuracy of the procedure. The results are herein summarised:

- The initial stiffness is predicted within an error range that reduces from (− 75%, 35%) for 2-storey cases to (− 15%, 15%) for 6-storey cases. For the Beam-Sway and Mixed-Sway mechanisms, it is under-predicted for uniform infills distribution while over-estimated if pilotis. For Column-Sway cases, it is under predicted for the majority of the cases, and the error reduces increasing the number of storeys;
- The peak base shear is predicted with a particularly small error for Column-Sway cases (− 0.1%, 3.3%), with the exception of a few case studies with weak infills. The error falls in the interval (− 5%, 20%) for the majority of the Beam-Sway and Mixed-Sway cases;
- The ultimate displacement is over-estimated (about 20% maximum) for Beam-Sway cases with 2 or 4 storeys while the error is higher for 6-storeys cases (40% over-estimation, on average). For Mixed-Sway mechanisms, this error falls in the interval (− 20%, 20%): over-prediction is seen for 2- and 4-storeys cases while there is under-prediction for 6-storeys cases. For Column-Sway cases, the error falls in the interval (− 20%, 35%), with over-prediction observed for all the cases except the 6-storeys ones, for which 10% mean under-prediction is observed;
- The ultimate base shear is under-predicted for all the analysed Beam-Sway cases (20%, on average) since the hardening of the members is conservatively not considered in SLaMA. An error within the interval (− 5%, 20%) is seen for Mixed-Sway mechanisms, with greater dispersion observed for the 2-storey cases. The error is close to zero for the pilotis Column-Sway cases while a 20% maximum under-prediction is observed for uniformly-infilled cases.

Overall, it is deemed that the proposed procedure is a reliable and accurate analyti- cal method to effectively provide a first estimation of the capacity of RC infilled frame

structures in a particularly simple way and without the need of any numerical analysis. The out-of-plane response of the infills is not currently considered within the procedure. Given the significance of this aspect, further investigations are required.

Acknowledgements This study was performed in the framework of the "SAFER Concrete Technology" and "Advancements in Engineering Guidelines and Standards" projects, funded by the New Zealand Natural Hazard Research Platform (NHRP) and of the PE 2014–2018 joint program DPC (Italian Department of Civil Protection)—ReLUIS (Laboratories University Network of Seismic Engineering).

References

Asteris PG, Chrysostomou CZ, Giannopoulos IP, Smyrou E (2011) Masonry infilled reinforced concrete frames with openings. In: III ECCOMAS thematic conference on computational methods in structural dynamics and earthquake engineering, Corfu, Greece, May 2011

Asteris PG, Giannopoulos IP, Chrysostomou CZ (2012) Modeling of infilled frames with openings. Open Constr Build Technol J 6:81–91

Asteris PG, Cotsovos DM, Chrysostomou CZ, Mohebkhah A, Al-Chaar GK (2013) Mathematical micro-modeling of infilled frames: state of the art. Eng Struct 56:1905–1921

Asteris PG, Cavaleri L, Di Trapani F, Sarhosis V (2016) A macro-modelling approach for the analysis of infilled frame structures considering the effects of openings and vertical loads. Struct Infrastruct Eng 12(5):551–566

ATC 40 (1996) Applied technology council. Seismic evaluation and retrofit of concrete buildings, Redwood City

Bertoldi SH, Decanini LD, Gavarini C (1993) Telai tamponati soggetti ad azione sismica, un modello semplificato: confronto sperimentale e numerico (in Italian). In: Proceedings of the VI Italian conference on seismic engineering (ANIDIS). Perugia, Italy

Cardone D, Flora A (2017) Multiple inelastic mechanisms analysis (MIMA): a simplified method for the estimation of the seismic response of RC frame buildings. Eng Struct 145:368–380

Carr AJ (2016) *RUAUMOKO2D*—The Maori God of volcanoes and earthquakes. Inelastic Analysis Finite Element program, Christchurch

Cavaleri L, Di Trapani F (2015) Prediction of the additional shear action on frame members due to infills. Bull Earthq Eng 13(5):1425–1454

Chrysostomou CZ, Asteris PG (2012) On the in-plane properties and capacities of infilled frames. Eng Struct 41:385–402

Crisafulli FJ (1997) Seismic behaviour of reinforced concrete structures with masonry infills. Ph.D. the- sis, Department of Civil Engineering and Natural Resources, University of Canterbury, Christch- urch, New Zealand

Crisafulli FJ, Carr AJ, Park R (2000) Analytical modelling of infilled frames structures: a general review. Bull N Z Soc Earthq Eng 33(1):30–47

De Luca F, Woods GED, Galasso C, D'Ayala D (2018) RC infilled building performance against the evidence of the 2016 EEFIT Central Italy post-earthquake reconnaissance mission: empirical fragilities and comparison with the FAST method. Bull Earthq Eng 16:2943–2969. https://doi.org/10.1007/s10518-017-0289-1

Del Vecchio C, Gentile R, Di Ludovico M, Uva G, Pampanin S (2018) Implementation and validation of the simple lateral mechanism analysis (SLaMA) for the seismic performance assessment of a dam- aged case study building. J Earthq Eng. https://doi.org/10.1080/13632469.2018.1483278

EC8, European Committee for Standardisation (CEN) (2005) Eurocode 8: design of structures for earthquake resistance Part 3: strengthening and repair of buildings. Belgium, Brussels

Furtado A, Rodrigues H, Arêde A, Varum H, Grubišić M, Šipoš TK (2018a) Prediction of the earth- quake response of a three-storey infilled RC structure. Eng Struct 171:214–235

Furtado A, Rodrigues H, Arêde A, Varum H (2018b) Out-of-plane behavior of masonry infilled RC frames based on the experimental tests available: a systematic review. Constr Build Mater 168:831–848

Gentile R (2017) Extension, refinement and validation of the simple lateral mechanism analysis (SLaMA) for the seismic assessment of RC structures. PhD thesis, Department of Civil, Environmental and Landscape, Building Engineering and Chemistry, Polytechnic University of Bari, Bari, Italy

Gentile R, Del Vecchio C, Pampanin S (2017) Seismic assessment of a RC case study building using the simple lateral mechanism analysis, SLaMA, method. In: 6th ECCOMAS thematic conference on computational methods in structural dynamics and earthquake engineering. Rhodes Island, Greece, 15–17 June 2017

Gentile R, Uva G, Pampanin S (2018) Mechanical interpretation of infills-to-frame interaction: contributions to the global base shear for strut-based frame models. In: 16th European conference on earth-

quake engineering (16ECEE). Thessaloniki, Greece, 18–21 June 2018
Gentile R, Del Vecchio C, Pampanin S, Raffaele D, Uva G (2019a) Refinement and validation of the Simple Lateral Mechanism Analysis (SLaMA) procedure for RC bare frames. J Earthq Eng. https://doi.org/10.1080/13632469.2018.1560377
Gentile R, Pampanin S, Raffaele D, Uva G (2019b) Non-linear analysis of RC masonry-infilled frames using the SLaMA method. Part 1: mechanical interpretation of the infill/frame interaction and formulation of the procedure. Bull Earthq Eng (**in press**)
Holmes M (1961) Steel frames with brickwork and concrete infilling. ICE Proc 19(4):473–478
King DJ, Priestley MJN, Park R (1986) Computer programs for concrete column design. Research report 86/12, Department of Civil Engineering
Kowalsky MJ, Priestley MJN (2000) Improved analytical model for shear strength of circular reinforced concrete columns in seismic regions. ACI Struct J 97:388–396
Landi L, Tardini A, Diotallevi PP (2016) A procedure for the displacement-based seismic assessment of infilled RC frames. J Earthq Eng 20(7):1077–1103
Magenes G, Pampanin S (2004) Seismic response of gravity-load design frames with masonry infills. In: 13th world conference on earthquake engineering
Mander JB, Priestley MJN, Park R (1988) Theoretical stress strain model for confined concrete. J Struct Eng 114(8):1804–1826
Montejo LA, Kowalsky MJ (2007) Set of codes for the analysis of reinforced concrete members. Raleigh, North Carolina
Morandi P, Hak S, Magenes G (2011) Comportamento sismico delle tamponature in laterizio in telai in C. A.: definizione dei livelli prestazionali e calibrazione di un modello numerico (in Italian). In: XIV Convegno 'l'ingegneria sismica in Italia' (ANIDIS)
NZSEE New Zealand Society for Earthquake Engineering (2017) The seismic assessment of existing buildings—technical guidelines for engineering assessments. Wellington, New Zealand
Pampanin S, Kam WY, Akguzel U, Tasligedik AS, Quintana Gallo P (2012) Seismic performance of reinforced concrete buildings in the christchurch CBD in 22 February 2011 earthquake. In: Part I: overview, University of Canterbury, Christchurch, New Zealand
Park R (1995) A static force-based procedure for the seismic assessment of existing reinforced concrete moment resisting frames. Bull N Z Soc Earthq Eng 30(3):213–226
Priestley MJN (1997) Displacement-based seismic assessment of reinforced concrete buildings. J Earthq Eng 1(1):157–192
Priestley MJN, Calvi G (1991) Towards a capacity-design assessment procedure for reinforced concrete frames. Earthq Spectra 7(3):413–437
Priestley MJN, Calvi GM, Kowalsky MJ (2007) Displacement-based seismic design of structures. IUSS Press, Pavia
Ricci P, Di Domenico M, Verderame GM (2018) Empirical-based out-of-plane URM infill wall model accounting for the interaction with in-plane demand. Earthquake Eng Struct Dyn 47:802–827
Santhi MH, Knight GMS, Muthumani K (2005) Evaluation of seismic response of soft-storey infilled frames. Computers and Concrete 2(6):423–437
Sharpe RD (1976) The seismic response of inelastic structures. PhD thesis, Department of Civil Engineering, University of Canterbury, Christchurch, New Zealand